Lawrence Berkeley National Laboratory
Lawrence Berkeley National Laboratory

Title

Midrapidity Lambda and [bar]Lambda production in Au + Au collisions at square root S=130 GeV

Permalink

https://escholarship.org/uc/item/8z36j9b8

Authors

Adler, C.
Ahammed, Z.
Allgower, C.
et al.

Publication Date

2002-03-22

Mid-rapidity Λ and $\overline{\Lambda}$ Production in Au+Au Collisions at $\sqrt{s_{NN}} = 130$ GeV

C. Adler[11], Z. Ahammed[23], C. Allgower[12], J. Amonett[14], B.D. Anderson[14], M. Anderson[5], G.S. Averichev[9], J. Balewski[12], O. Barannikova[9,23], L.S. Barnby[14], J. Baudot[13], S. Bekele[20], V.V. Belaga[9], R. Bellwied[31], J. Berger[11], H. Bichsel[30], L.C. Bland[2], C.O. Blyth[3], B.E. Bonner[24], A. Boucham[26], A. Brandin[18], A. Bravar[2], R.V. Cadman[1], H. Caines[20], M. Calderón de la Barca Sánchez[2], A. Cardenas[23], J. Carroll[15], J. Castillo[26], M. Castro[31], D. Cebra[5], P. Chaloupka[20], S. Chattopadhyay[31], Y. Chen[6], S.P. Chernenko[9], M. Cherney[8], A. Chikanian[33], B. Choi[28], W. Christie[2], J.P. Coffin[13], T.M. Cormier[31], J.G. Cramer[30], H.J. Crawford[4], W.S. Deng[2], A.A. Derevschikov[22], L. Didenko[2], T. Dietel[11], J.E. Draper[5], V.B. Dunin[9], J.C. Dunlop[33], V. Eckardt[16], L.G. Efimov[9], V. Emelianov[18], J. Engelage[4], G. Eppley[24], B. Erazmus[26], P. Fachini[2], V. Faine[2], K. Filimonov[15], E. Finch[33], Y. Fisyak[2], D. Flierl[11], K.J. Foley[2], J. Fu[15,32], C.A. Gagliardi[27], N. Gagunashvili[9], J. Gans[33], L. Gaudichet[26], M. Germain[13], F. Geurts[24], V. Ghazikhanian[6], O. Grachov[31], V. Grigoriev[18], M. Guedon[13], E. Gushin[18], T.J. Hallman[2], D. Hardtke[15], J.W. Harris[33], T.W. Henry[27], S. Heppelmann[21], T. Herston[23], B. Hippolyte[13], A. Hirsch[23], E. Hjort[15], G.W. Hoffmann[28], M. Horsley[33], H.Z. Huang[6], T.J. Humanic[20], G. Igo[6], A. Ishihara[28], Yu.I. Ivanshin[10], P. Jacobs[15], W.W. Jacobs[12], M. Janik[29], I. Johnson[15], P.G. Jones[3], E.G. Judd[4], M. Kaneta[15], M. Kaplan[7], D. Keane[14], J. Kiryluk[6], A. Kisiel[29], J. Klay[15], S.R. Klein[15], A. Klyachko[12], A.S. Konstantinov[22], M. Kopytine[14], L. Kotchenda[18], A.D. Kovalenko[9], M. Kramer[19], P. Kravtsov[18], K. Krueger[1], C. Kuhn[13], A.I. Kulikov[9], G.J. Kunde[33], C.L. Kunz[7], R.Kh. Kutuev[10], A.A. Kuznetsov[9], L. Lakehal-Ayat[26], M.A.C. Lamont[3], J.M. Landgraf[2], S. Lange[11], C.P. Lansdell[28], B. Lasiuk[33], F. Laue[2], A. Lebedev[2], R. Lednický[9], V.M. Leontiev[22], M.J. LeVine[2], Q. Li[31], S.J. Lindenbaum[19], M.A. Lisa[20], F. Liu[32], L. Liu[32], Z. Liu[32], Q.J. Liu[30], T. Ljubicic[2], W.J. Llope[24], G. LoCurto[16], H. Long[6], R.S. Longacre[2], M. Lopez-Noriega[20], W.A. Love[2], T. Ludlam[2], D. Lynn[2], J. Ma[6], R. Majka[33], S. Margetis[14], C. Markert[33], L. Martin[26], J. Marx[15], H.S. Matis[15], Yu.A. Matulenko[22], T.S. McShane[8], F. Meissner[15], Yu. Melnick[22], A. Meschanin[22], M. Messer[2], M.L. Miller[33], Z. Milosevich[7], N.G. Minaev[22], J. Mitchell[24] V.A. Moiseenko[10], C.F. Moore[28], V. Morozov[15], M.M. de Moura[31], M.G. Munhoz[25], J.M. Nelson[3], P. Nevski[2], V.A. Nikitin[10], L.V. Nogach[22], B. Norman[14], S.B. Nurushev[22], G. Odyniec[15], A. Ogawa[21], V. Okorokov[18], M. Oldenburg[16], D. Olson[15], G. Paic[20], S.U. Pandey[31], Y. Panebratsev[9], S.Y. Panitkin[2], A.I. Pavlinov[31], T. Pawlak[29], V. Perevoztchikov[2], W. Peryt[29], V.A Petrov[10], M. Planinic[12], J. Pluta[29], N. Porile[23], J. Porter[2], A.M. Poskanzer[15], E. Potrebenikova[9], D. Prindle[30], C. Pruneau[31], J. Putschke[16], G. Rai[15], G. Rakness[12], O. Ravel[26], R.L. Ray[28], S.V. Razin[9,12], D. Reichhold[8], J.G. Reid[30], F. Retiere[15], A. Ridiger[18], H.G. Ritter[15], J.B. Roberts[24], O.V. Rogachevski[9], J.L. Romero[5], C. Roy[26], V. Rykov[31], I. Sakrejda[15], S. Salur[33], J. Sandweiss[33], A.C. Saulys[2], I. Savin[10], J. Schambach[28], R.P. Scharenberg[23], N. Schmitz[16], L.S. Schroeder[15], A. Schüttauf[16], K. Schweda[15], J. Seger[8], D. Seliverstov[18], P. Seyboth[16], E. Shahaliev[9], K.E. Shestermanov[22], S.S. Shimanskii[9], V.S. Shvetcov[10], G. Skoro[9], N. Smirnov[33], R. Snellings[15], P. Sorensen[6], J. Sowinski[12], H.M. Spinka[1], B. Srivastava[23], E.J. Stephenson[12], R. Stock[11], A. Stolpovsky[31], M. Strikhanov[18], B. Stringfellow[23], C. Struck[11], A.A.P. Suaide[31], E. Sugarbaker[20], C. Suire[2], M. Šumbera[20], B. Surrow[2], T.J.M. Symons[15], A. Szanto de Toledo[25], P. Szarwas[29], A. Tai[6], J. Takahashi[25], A.H. Tang[14], J.H. Thomas[15], M. Thompson[3], V. Tikhomirov[18], M. Tokarev[9], M.B. Tonjes[17], T.A. Trainor[30], S. Trentalange[6], R.E. Tribble[27], V. Trofimov[18], O. Tsai[6], T. Ullrich[2], D.G. Underwood[1], G. Van Buren[2], A.M. VanderMolen[17], I.M. Vasilevski[10], A.N. Vasiliev[22], S.E. Vigdor[12], S.A. Voloshin[31], F. Wang[23], H. Ward[28], J.W. Watson[14], R. Wells[20], G.D. Westfall[17], C. Whitten Jr.[6], H. Wieman[15], R. Willson[20], S.W. Wissink[12], R. Witt[32], J. Wood[6], N. Xu[15], Z. Xu[2], A.E. Yakutin[22], E. Yamamoto[15], J. Yang[6], P. Yepes[24], V.I. Yurevich[9], Y.V. Zanevski[9], I. Zborovský[9], H. Zhang[33], W.M. Zhang[14], R. Zoulkarneev[10], A.N. Zubarev[9]

(STAR Collaboration)

[1] *Argonne National Laboratory, Argonne, Illinois 60439*
[2] *Brookhaven National Laboratory, Upton, New York 11973*
[3] *University of Birmingham, Birmingham, United Kingdom*
[4] *University of California, Berkeley, California 94720*
[5] *University of California, Davis, California 95616*
[6] *University of California, Los Angeles, California 90095*
[7] *Carnegie Mellon University, Pittsburgh, Pennsylvania 15213*
[8] *Creighton University, Omaha, Nebraska 68178*
[9] *Laboratory for High Energy (JINR), Dubna, Russia*
[10] *Particle Physics Laboratory (JINR), Dubna, Russia*

[11] *University of Frankfurt, Frankfurt, Germany*
[12] *Indiana University, Bloomington, Indiana 47408*
[13] *Institut de Recherches Subatomiques, Strasbourg, France*
[14] *Kent State University, Kent, Ohio 44242*
[15] *Lawrence Berkeley National Laboratory, Berkeley, California 94720*
[16] *Max-Planck-Institut fuer Physik, Munich, Germany*
[17] *Michigan State University, East Lansing, Michigan 48824*
[18] *Moscow Engineering Physics Institute, Moscow Russia*
[19] *City College of New York, New York City, New York 10031*
[20] *Ohio State University, Columbus, Ohio 43210*
[21] *Pennsylvania State University, University Park, Pennsylvania 16802*
[22] *Institute of High Energy Physics, Protvino, Russia*
[23] *Purdue University, West Lafayette, Indiana 47907*
[24] *Rice University, Houston, Texas 77251*
[25] *Universidade de Sao Paulo, Sao Paulo, Brazil*
[26] *SUBATECH, Nantes, France*
[27] *Texas A & M, College Station, Texas 77843*
[28] *University of Texas, Austin, Texas 78712*
[29] *Warsaw University of Technology, Warsaw, Poland*
[30] *University of Washington, Seattle, Washington 98195*
[31] *Wayne State University, Detroit, Michigan 48201*
[32] *Institute of Particle Physics, Wuhan, Hubei 430079 China and*
[33] *Yale University, New Haven, Connecticut 06520*
(Dated: March 22, 2002)

We report the first measurement of strange (Λ) and anti-strange ($\overline{\Lambda}$) baryon production from $\sqrt{s_{NN}} = 130$ GeV Au+Au collisions at the Relativistic Heavy Ion Collider (RHIC). Rapidity density and transverse mass distributions at mid-rapidity are presented as a function of centrality. The yield of Λ and $\overline{\Lambda}$ hyperons is found to be approximately proportional to the number of negative hadrons. The production of $\overline{\Lambda}$ hyperons relative to negative hadrons increases very rapidly with transverse momentum. The magnitude of the increase cannot be described by existing hadronic string fragmentation models.

Ultra-relativistic nucleus-nucleus collisions provide a unique means to create nuclear matter of high energy density (temperature) and/or baryon density over an extended volume [1]. The first results from the Relativistic Heavy Ion Collider (RHIC) have shown that the large charged particle multiplicity, measured in Au+Au collisions at $\sqrt{s_{NN}} = 130$ GeV, corresponds to an energy density significantly higher than that previously achieved in heavy ion collisions [2, 3, 4]. In addition, the anti-proton to proton ratio at mid-rapidity has been measured to be in the range 0.6–0.7 [5, 6, 7], which is indicative of particle production from a low net baryon density regime. Thus the global characteristics of nucleus-nucleus collisions at RHIC are the formation of a high energy density and low net baryon density region at mid-rapidity.

The yield of baryons and anti-baryons produced in relativistic nuclear collisions is very important because it is sensitive to two fundamental, not yet fully understood aspects of hadron production dynamics: baryon/anti-baryon pair production and the transport of baryon number from beam rapidity to mid-rapidity. The nature of baryon/anti-baryon production itself is the subject of much interest, with theoretical conjecture addressing a range of possible mechanisms from string fragmentation [8], to exotic mechanisms involving Quantum Chromo Dynamics (QCD) domain walls [9]. The physical nature of the entity which carries baryon number, and the means by which baryon number is transported over a large rapidity gap into the mid-rapidity region are also subjects of considerable experimental and theoretical interest [10, 11, 12].

Strange baryon/anti-baryon production is particularly interesting due to the increased sensitivity to the availability of strange/anti-strange quarks, which is expected to be suppressed relative to light quarks in hadronic matter due to the strange quark mass. Strangeness production has long been predicted to be a signature of Quark Gluon Plasma (QGP) formation [13]. The strangeness production in previous generations of heavy ion experiments has been observed to be significantly increased compared to those from p+p, p+A and light ion collisions [14, 15, 16, 17], although questions remain about the exact strangeness production mechanism. In particular, the relative importance of strange baryon production from hadronic rescattering differs between calculations [18, 19], depending on both the evolution of the system and the scattering cross sections assumed. Exotic dynamical mechanisms that have been proposed for strange baryon production include, for example, Color String Ropes [20], String Fusion [21] and Multi-mesonic

Reactions [22]. All require a high local energy density and therefore suggest that strangeness production occurs early in the collision.

In this letter we report on mid-rapidity ($|y|<0.5$) Lambda (Λ) and anti-Lambda ($\overline{\Lambda}$) production in Au+Au collisions at $\sqrt{s_{NN}} = 130$ GeV. The data were taken with the STAR (Solenoidal Tracker At RHIC) detector. The main components of the detector system for this analysis have been described in detail elsewhere [23]. They included a large volume Time-Projection Chamber (TPC) [24], a pair of Zero-Degree Calorimeters (ZDC) located at +/- 18 meters from the center of the TPC, and a Central Trigger Barrel (CTB) constructed of scintillator paddles surrounding the TPC.

The TPC was used to provide tracking information and particle identification by measuring the specific ionization loss (dE/dx) for charged particles. The ZDCs were used in coincidence to define a minimum bias trigger by selecting interactions from the intersection region of the colliding beams, and to measure the forward going energy of near-beam rapidity fragments, consisting primarily of spectator neutrons. The CTB was used to define a central interaction trigger based on the energy deposition from charged particles entering its acceptance.

Data from both the minimum bias trigger and central trigger have been used for this analysis. Similar to a previous analysis [4], the collision centrality was defined off-line using the total charged particle multiplicity within a pseudo-rapidity window of $|\eta| < 0.5$. The charged particle multiplicity distribution was divided into five centrality bins, corresponding to approximately the most central 5%, 5–10%, 10–20%, 20–35%, 35–75% of the total hadronic inelastic cross section of Au+Au collisions.

The Λ and $\overline{\Lambda}$ particles were reconstructed from their weak decay topology, $\Lambda \to p\pi^-$ and $\overline{\Lambda} \to \overline{p}\pi^+$, using charged tracks measured in the TPC. These tracks were projected back from the TPC to find their Distance of Closest Approach (DCA) to the primary vertex. Since the tracks of particles from Λ and $\overline{\Lambda}$ decays should not originate from the primary vertex, only proton (anti-proton) candidate tracks missing the primary vertex by 0.90 cm and π^- (π^+) candidate tracks missing the primary vertex by 2.85 cm were selected. Particle assignments for p ($\overline{p}$) and π^- (π^+) candidates were based on charge sign and the mean energy loss, $<dE/dx>$, measured for each track. Candidate tracks were then paired to form neutral decay vertices, which were required to be at least 5 cm from the primary vertex. The momentum vector of the reconstructed parent particle was required to originate from the primary interaction: the distance of closest approach of the parent trajectory to the primary vertex was required to be less than 0.5 cm. The effect of these cuts on the reconstruction efficiency was determined using the embedding techniques described below.

Figure 1 shows the invariant mass distributions for the reconstructed Λ and $\overline{\Lambda}$ candidates in $|y| < 0.5$ for two typ-
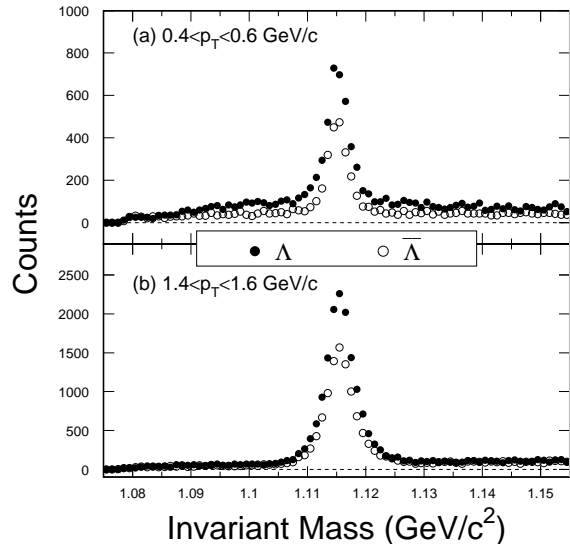

FIG. 1: Invariant mass distribution of Λ (solid-circles) and $\overline{\Lambda}$ (open-circles) candidates from the data sample analyzed including both central and minimum-bias collisions: (a) $0.4 < p_T < 0.6$ GeV/c; (b) $1.4 < p_T < 1.6$ GeV/c

ical p_T bins from the data sample. The mass resolutions (σ) for reconstructed Λ and $\overline{\Lambda}$ are typically about 3–4 MeV/c^2 based on a Gaussian fit to the peak. The background beneath the $\Lambda(\overline{\Lambda})$ peak is dominated by combinatoric pairs of charged particles. Decays of $K_s^0 \to \pi^+\pi^-$ also contribute to the smooth background due to pions misidentified as protons. The yield is obtained from the invariant mass distribution in each transverse momentum (p_T) and rapidity (y) bin, where the shape of the background near the $\Lambda(\overline{\Lambda})$ peak is fit with a second order polynomial function. The signal to background ratios in the peak are greater than 6 for all the measured p_T bins. Variations in the yield due to different fits for the background have been included in the estimate of systematic errors.

The raw yield for each p_T-y bin was then corrected for finite detection efficiency. The overall correction factor was obtained from a Monte Carlo embedding procedure. $\Lambda(\overline{\Lambda})$ particles were generated using a STAR GEANT package for detector simulation including all physical processes to take into account effects such as scattering and absorption in the detector support structures. A TPC Response Simulator (TRS) was used to generate TPC information at the pad level for all charged tracks inside the TPC from simulated Λ and $\overline{\Lambda}$ decays. The TRS includes all TPC resolution effects ranging from electron transport in the gas to signal processing in the readout electronics. The simulated data were then embedded into real collision events from STAR detectors and were analyzed with the standard STAR software package as real data. The correction factor for each p_T-y and multiplic-

ity bin was obtained from the number of Λ ($\overline{\Lambda}$) particles reconstructed from the embedded sample, divided by the number generated. The combined acceptance and efficiency for Λ and $\overline{\Lambda}$ ranges from 0.8% to 5.8% as a function of p_T for the most central collision sample.
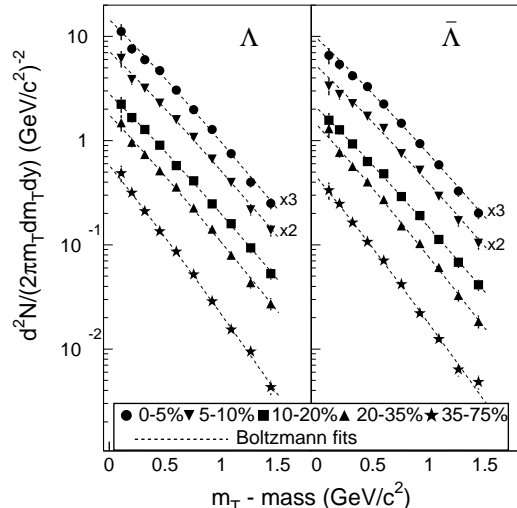
Centrality		0–5%	5–10%	10–20%	20–35%	35–75%
dN/dy	Λ	17.0±0.4	13.0±0.3	10.1±0.2	5.9±0.2	1.61±0.05
(Boltz)	$\overline{\Lambda}$	12.0±0.3	9.6±0.3	7.4±0.2	4.6±0.1	1.26±0.04
T_B	Λ	298±5	304±6	303±6	289±6	254±5
(MeV)	$\overline{\Lambda}$	312±6	310±6	305±6	280±6	258±5
dN/dy	Λ	17.4±0.4	13.3±0.3	10.4±0.2	6.1±0.2	1.66±0.05
(exp fit)	$\overline{\Lambda}$	12.3±0.3	9.8±0.3	7.6±0.2	4.7±0.1	1.30±0.04
T_E	Λ	355±8	364±9	362±8	343±8	295±7
(MeV)	$\overline{\Lambda}$	374±9	373±8	366±8	331±8	301±7

TABLE I: Fit parameters from Boltzmann and exponential fits of the m_T spectra for Λ and $\overline{\Lambda}$ at mid-rapidity ($|y|<0.5$). Only statistical errors are presented. The systematic errors on dN/dy and T are approximately 10%.

FIG. 2: Transverse mass distributions of Λ (left) and $\overline{\Lambda}$ (right) at mid-rapidity ($|y|<0.5$) for selected centrality bins. The dashed lines are Boltzmann fits. Note that multiplicative factors have been applied to data from the two most central data sets for display.
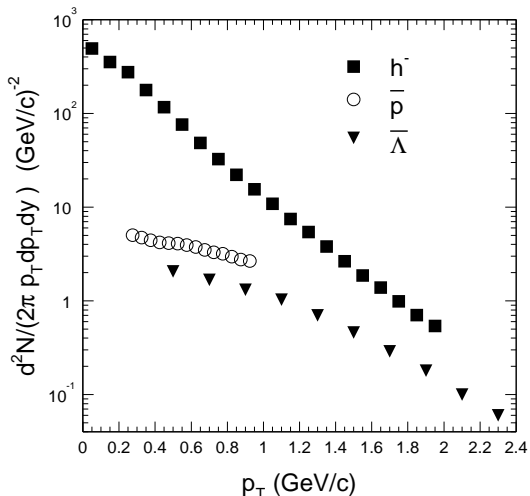

FIG. 3: The mid-rapidity $\overline{\Lambda}$ ($|y|<0.5$) transverse momentum distribution from the top 5% most central collisions. For comparison the distributions for negative hadrons ($d^2N/(2\pi p_T)dp_Td\eta$, $|\eta|<0.1$) and anti-protons ($|y|<0.1$) for the similar centrality bin are included. Statistical errors are less than the size of the data points.

The measured Λ spectra contain contributions from primordial Λ, Σ^0 decays, and feed-down from multiply-strange hyperons–notably Ξ^0 and Ξ^-. The primordial Λ and the Σ^0 decay products cannot be separated in our analysis and have been treated as primary Λ. We have investigated the feed-down from Ξ hyperons by comparing systematically the distribution of the DCA to the primary interaction vertex for the reconstructed Λ from real data versus simulated primary Λ and secondary Λ from Ξ decay. From this analysis, we estimate the contributions of feed-down from multiply-strange hyperons, mostly Ξ and $\overline{\Xi}$ decays, to be approximately $(27 \pm 6)\%$ of the measured Λ and $\overline{\Lambda}$ yields respectively.

Figure 2 presents the m_T spectra (invariant distributions) of Λ and $\overline{\Lambda}$ for five selected centrality bins. Systematic errors from various methods of yield extraction, reconstruction efficiencies and uncorrected sector-by-sector variations in the TPC performance are included. Both exponential ($e^{-(m_T-m)/T_E}$) and Boltzmann ($m_T e^{-(m_T-m)/T_B}$) functions, as well as a Gaussian ($e^{-p_T^2/(2\sigma^2)}$) in p_T have been used to fit the data, following the ansatz described in [25].

All three functional forms were fit to the Λ and $\overline{\Lambda}$ spectra used for this analysis. The slope parameter obtained from the exponential fit is systematically higher than that for the Boltzmann by approximately 40–65 MeV. However, overall the integrated yields from all three fit functions are consistent within the statistical errors. The slope parameters and the dN/dy for the Boltzmann and exponential fits are presented in Table I. The Boltzmann form was adopted in Figure 2 because it typically provides a better χ^2 and gives a reasonable description of the m_T spectra over the entire range of centrality and tranverse momenta investigated.

Within the systematic error, the slope parameters measured for the Λ and $\overline{\Lambda}$ m_T distributions are the same. There is a systematic increase in the slope parameters from approximately 254 MeV for the least central (35-75%) to 312 MeV for the most central (0-5%) bin. Sim-

ilar behavior as a function of centrality is found for the $\overline{p}$ transverse mass distributions [25]. Assuming the temperature at which particle interactions cease (the "freeze-out temperature [26]) is constant independent of collision centrality, the increase in the slope parameter may be interpreted as an increase in the collective radial velocity [27, 28].

A possible indication of hydrodynamic flow is the increase of the observed mean transverse momenta for various species with increasing particle mass. The transverse momentum distributions of negatively charged hadrons, as well as $\overline{p}$ and $\overline{\Lambda}$ are shown in Figure 3. The $\overline{p}$ and $\overline{\Lambda}$ p_T distributions are similar in shape in the region where they can be compared (below 1 GeV/c), even though the data sets cover somewhat different ranges in p_T. Both distributions are qualitatively different from and much less steep than the corresponding h$^-$ distribution, which is dominated by pions. Qualitatively similar behavior was observed in heavy ion collisions at the CERN Super Proton Synchrotron (SPS) [27, 28, 29]. In general, the slope parameters for all species are observed to be larger at RHIC, which is attributed to an increase in the collective radial velocity as a function of center-of-mass energy [30].

Figure 3 indicates that at higher p_T (p_T>1 GeV/c) the ratio of $\overline{\Lambda}$ to negative hadrons increases rapidly. The baryon to meson ratio at RHIC for p_T>1 GeV/c exceeds expectations from perturbative QCD inspired string fragmentation models which were tuned to fit e^+e^- collision data and are the basis for modeling particle production in hadronic collisions as well [8, 31, 32]. For example, the $\overline{\Lambda}$ to h$^-$ ratio is approximately 0.35 at p_T of 2 GeV/c. Data from e^+e^- collisions and calculations from string fragmentation models, however, indicate that although the baryon to meson ratio from quark and gluon fragmentation increases as a function of Feynman x, the ratio never exceeds 0.2 [33]. As mentioned above, a natural explanation for the increase at high p_T would be a large collective radial flow at RHIC [26, 29]. Alternatively, it has also been suggested that the energy loss of high p_T partons could modify the baryon to meson ratio [31]. To determine the exact dynamics that cause the relative enhancement of baryons to mesons at high p_T, more experimental measurements over a larger p_T-range are needed.

The average ratio of p_T integrated yield $\overline{\Lambda}$ to Λ is 0.74± 0.04 with no significant variation over the measured range of centrality. Given that there is a net excess of baryons at mid-rapidity, it is reasonable to conclude that there is more than one process contributing to Λ production and that significant baryon number from the colliding beams is transported to Λ hyperons at mid-rapidity. A question in that regard is why the shapes of m_T spectra for Λ and $\overline{\Lambda}$ are the same within errors. It has been suggested that significant rescattering of Λ and $\overline{\Lambda}$ during the evolution of the collision can lead to equilibration [19, 34]. The

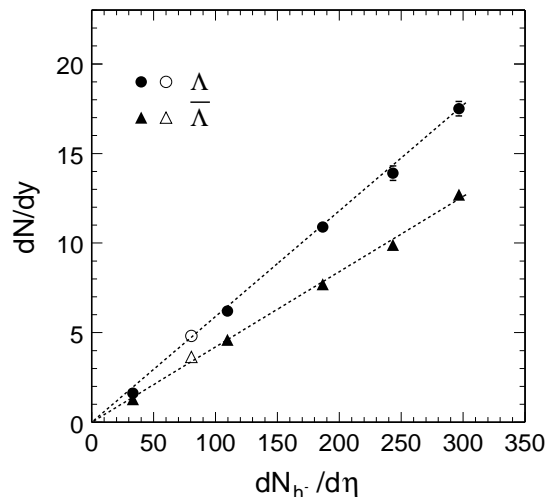FIG. 4: Λ and $\overline{\Lambda}$ rapidity density as a function of negative hadron multiplicity at mid-rapidity. The open symbols in the figure are data points from an independent analysis of minimum bias data set using event-mixing techniques. Errors shown are statistical only.

nature of baryon number transport itself requires further study.

Figure 4 shows the dN/dy of Λ and $\overline{\Lambda}$ from the Boltzmann fit as a function of the h$^-$ pseudo-rapidity density [4]. At mid-rapidity the hyperon production is approximately proportional to the primary h$^-$ multiplicity in Au+Au collisions at RHIC. The dashed lines in the figure correspond to $\Lambda = (0.054 \pm 0.001)h^-$ and $\overline{\Lambda} = (0.040 \pm 0.001)h^-$ from a linear fit to the data. Similar centrality dependence of the lambda production was observed at the SPS energies. The $\overline{\Lambda}$ to h$^-$ ratio at RHIC is much larger than that at the SPS while the Λ to h$^-$ ratio is smaller at RHIC [16]. This may be understood from the fact that at the SPS, most of the observed Λ hyperons carry baryon number transported from the colliding nuclei through associated production, rescattering and fragmentation processes. In this case, the yield of Λ to h$^-$ ratio is larger than that at RHIC due to the relatively high fraction of the Λ yield not resulting from pair production. Conversely, the increased importance of baryon pair production at RHIC energies must contribute to the observed increase of the $\overline{\Lambda}$ to h$^-$ ratio relative to the SPS measurement.

In conclusion, we have presented the first inclusive mid-rapidity ($|y|$<0.5) Λ and $\overline{\Lambda}$ spectra as a function of centrality from Au+Au collisions at the $\sqrt{s_{NN}}$ = 130 GeV energy. Salient features of the data include 1) large slope parameters of transverse mass spectra probably resulting from increased collective radial velocity at RHIC, 2) similar shapes for Λ and $\overline{\Lambda}$ spectra despite the fact that a significant fraction of the Λ hyperons at mid-rapidity carry baryon number from the incoming nuclei while the

$\overline{\Lambda}$ hyperons are primarily pair produced, and 3) a significant increase in the $\overline{\Lambda}$ yield relative to negatively charged primary hadrons at moderate p_T above 1 GeV/c which cannot be described by existing perturbative QCD inspired string fragmentation models. The p_T integrated rapidity densities of Λ and $\overline{\Lambda}$ are approximately proportional to the number of negative hadrons at mid-rapidity.

[1] J.P. Blaizot, Nucl. Phys. **A661**, 3c (1999) and references therein.
[2] B.B. Back *et al.*, Phys. Rev. Lett. **85**, 3100 (2000).
[3] K. Adcox *et al.*, Phys. Rev. Lett. **86**, 3500 (2001).
[4] C. Adler *et al.*, Phys. Rev. Lett. **87**, 112303 (2001).
[5] C. Adler *et al.*, Phys. Rev. Lett. **86**, 4778 (2001).
[6] B.B. Back *et al.*, Phys. Rev. Lett., **87**, 102301 (2001).
[7] I.G. Bearden *et al.*, Phys. Rev. Lett. **87**, 112305 (2001).
[8] B. Andersson *et al.*, Physica Scripta **32**, 574 (1985).
[9] J. Ellis *et al.*, Phys. Lett. **B233**, 223 (1989).
[10] W. Busza and R. Ledoux, Ann. Rev. of Nucl. and Part. Sci. **38**, 119 (1988).
[11] H.Z. Huang, Proceedings of Relativistic Heavy Ion Symposium APS Centennial Meeting '99, R. Seto, Editor. 3 (1999).
[12] D. Kharzeev, Phys. Lett. **B378**, 238 (1996).
[13] J. Rafelski and B. Müller, Phys. Rev. Lett. **48**, 1066 (1982); **56**, 2334(E) (1986).
[14] T. Abbott *et al.*, Phys. Rev. Lett. **64**, 847 (1990).
[15] S. Ahmad *et al.*, Phys. Lett. B**382**, 35 (1996).
[16] F. Antinori *et al.*, Eur. Phys. J. **C11**, 79 (1999).
[17] H. Appelshäuser *et al.*, Phys. Lett. **B444**, 523 (1998).
[18] P. Koch *et al.*, Phys. Rep. **142**, 167 (1986).
[19] R. Bellwied *et al.*, Phys. Rev. **C62**, 054906 (2000).
[20] H. Sorge, Phys. Rev. **C52**, 3291 (1995).
[21] N. Amelin *et al.*, Phys. Lett. **B306**, 312 (1993).
[22] R. Rapp and E. Shuryak, Phys. Rev. Lett. **86**, 2980 (2001).
[23] K.H. Ackermann *et al.*, Phys. Rev. Lett. **86**, 402 (2001).
[24] K.H. Ackermann *et al.*, Nucl. Phys. **A661**, 681c (1999).
[25] C. Adler *et al.*, Phys. Rev. Lett. 87, 262302 (2001) .
[26] E. Schnedermann, J. Sollfrank and U. Heinz, Phys. Rev. **C48**, 2462 (1993) .
[27] I. Bearden *et al.*, Phys. Rev. Lett. **78**, 2080 (1997) .
[28] H. Appelshäuser *et al.*, Eur. Phys. J. **C2**, 661 (1998) .
[29] H. van Hecke *et al.*, Phys. Rev. Lett. **81**, 5764 (1998).
[30] M. Kaneta and N. Xu, J. Phys. **G27**, 589 (2001).
[31] I. Vitev and M. Gyulassy, nucl-th/0104066.
[32] X.N. Wang, Phys. Rep. **280**, 287 (1997) .
[33] W. Hofmann, Ann. Rev. Nucl. Part. Sci. **38**, 279 (1988).
[34] P. Braun-Munzinger, D. Magestro, K. Redlich, and J. Stachel, Phys. Lett. **B518**, 41(2001).